Droplet Growth by Condensation and Coalescence in a Strong Updraft

H. G. LEIGHTON AND R. R. ROGERS

Dept. of Meteorology, McGill University, Montreal, Quebec, Canada

(Manuscript received 3 April 1973, in revised form 10 August 1973)

ABSTRACT

The growth of cloud droplets by condensation and coalescence in a strong updraft is investigated for different cloud conditions and different initial droplet distributions. Growth by coalescence is determined by solving the stochastic collection equation, and growth by condensation is calculated from the diffusion equation.

The results indicate that under suitable conditions, starting from an initial droplet distribution centered at about 8 μm radius with a dispersion of 0.2, an appreciable number of cloud droplets will grow to precipitation sizes in times of the order of 10–15 min. The results are sensitive to the initial droplet concentration and moisture content of the cloud. The importance of combining coalescence and condensation raises the question of the validity of calculations of rain formation by coalescence only.

1. Introduction

Twomey's (1966) analysis of the warm rain process rekindled interest in what is now called the stochastic coalescence equation, which describes the evolution of a cloud droplet spectrum by gravitational coalescence. Since then, a number of investigations of the coalescence process have been reported, which employ more accurate numerical techniques and more recent data on collision efficiencies (e.g., Berry, 1967; Warshaw, 1967, 1968; Bartlett, 1970; Reinhardt, 1972). In the meantime, others have asked whether the equation really describes the statistical effects which Twomey attributed to it (Scott, 1968b, c; Gillespie, 1972).

Notwithstanding the technical and theoretical uncertainties, a number of articles have appeared on precipitation development which employ the stochastic coalescence equation in one form or another. For example, Takeda's (1971) two-dimensional model of a precipitating convective cloud included a provision for coalescence among seven size-categories of drops. Srivastava (1971) used the equation in analyzing the evolution of raindrop spectra by coalescence and breakup, employing a logarithmic scale of radius in which the radius doubled every 12 categories. In an ambitious and important paper, Danielsen *et al.* (1972) modelled hail development in a one-dimensional, time-varying cloud model, including coalescence along with condensation, breakup, freezing, and other microphysical processes, with improved numerical accuracy. In a paper somewhat reminiscent of earlier work by East (1957), Kovetz and Olund (1969) analyzed droplet development by condensation and coalescence, concluding that the condensation induced by even a gentle updraft (10 cm sec^{-1}) causes the spectrum to change in such a way that coalescence is accelerated. Cotton (1972) integrated the equation, neglecting effects other than coalescence, to produce empirical data on the production of rain from cloud (autoconversion) to be used in a numerical cloud model.

In an attempt to describe precipitation development in the updraft region of a growing convective storm, we have calculated the development of a cloud droplet spectrum by condensation and coalescence, using the stochastic coalescence equation and a diffusional growth equation. In effect, we have isolated only a small fraction of the precipitation processes included in the comprehensive models of Takeda and Danielsen *et al.* Judging from the work of East and Kovetz and Olund, however, we were convinced of the important role played by condensation in promoting the coalescence process. Consequently, we examined the dependence of droplet development on updraft speed, the initial droplet spectrum, and cloud base temperature. The primary emphasis was on cases with a strong updraft, although calculations for weak and zero updrafts (i.e., no condensation) have been included for comparison.

2. The model

a. General description

A parcel of air containing cloud droplets is considered to rise in a uniform, constant updraft. A saturated adiabatic process is assumed. The temperature decreases approximately at the pseudoadiabatic rate and all condensed water remains with the parcel. The cloud droplets fall relative to each other with their

Unauthenticated | Downloaded 06/13/24 11:36 AM UTC

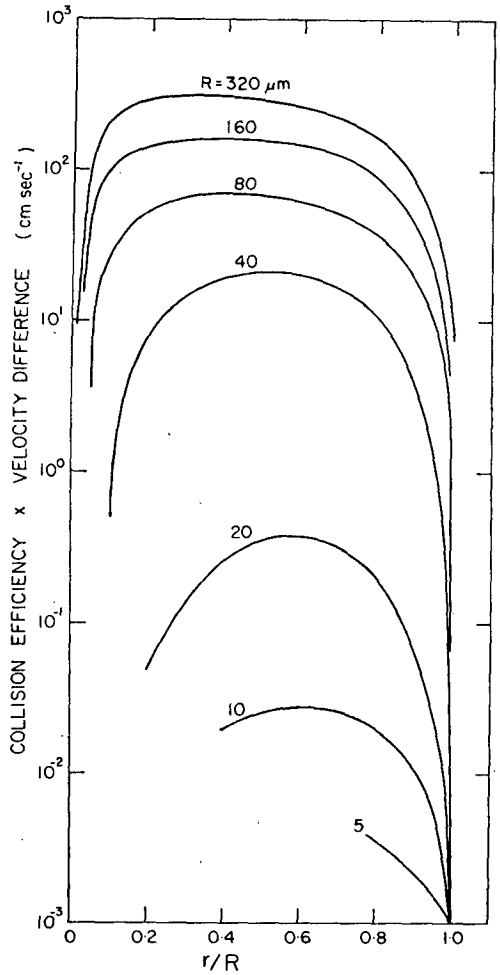

FIG. 1. Product of collision efficiency Y_c^2 and terminal velocity difference as a function of the ratio of the droplet radii, for different values of the radius of the larger drop.

terminal velocities, but do not leave the parcel. This assumption will be reasonable provided the terminal velocities are small compared to the updraft velocity.

The quantities specified are the parcel's initial temperature and pressure, the initial droplet spectrum, and the updraft speed. Equations describing the effects of condensation and gravitational coalescence are then integrated to give the form of the spectrum as a function of elapsed time or altitude. Mixing with ambient air is neglected and the amount of condensed water at any altitude is approximately given by the adiabatic liquid water content. The supersaturation at any time may be calculated, since it is proportional to condensation rate. The ice phase is neglected.

An important property of the model is that the droplet mixing ratio (number of drops per unit mass of air) does not change except as a result of coalescence. Thus, the effects of variations in supersaturation on the droplet mixing ratio are neglected. However, since the updraft is assumed constant, these effects are small.

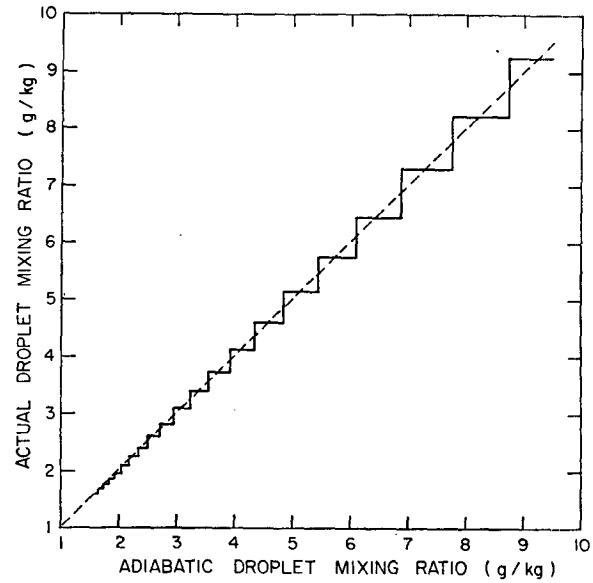

FIG. 2. A comparison of the droplet mixing ratio used in the calculations with the adiabatic value. The vertical steps in the solid curve occur at each condensation step and indicate the increase in water content. The dashed line is for an adiabatic mixing ratio.

The small droplets in the spectrum grow by condensation, and eventually coalescence, and are not replenished by the activation of more condensation nuclei or the mixing in of ambient cloudy air.

b. Coalescence

If $N(x)dx$ is the concentration of drops with masses between x and $x+dx$ then the stochastic equation de-

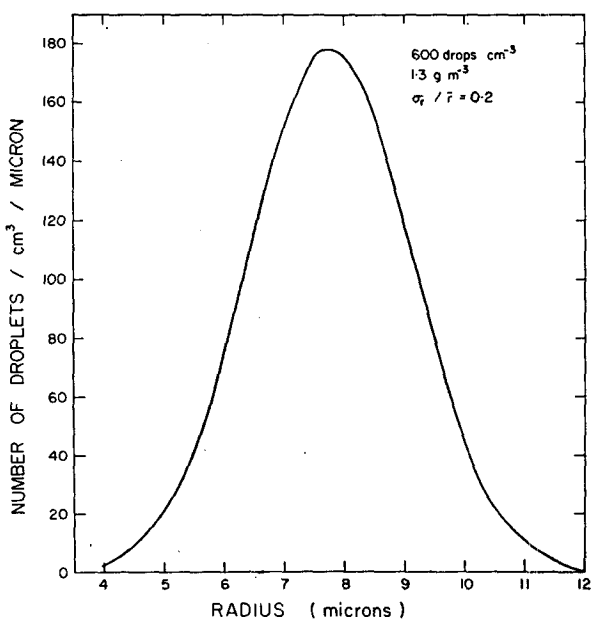

FIG. 3. Initial droplet distribution for the standard case.

Unauthenticated | Downloaded 06/13/24 11:36 AM UTC

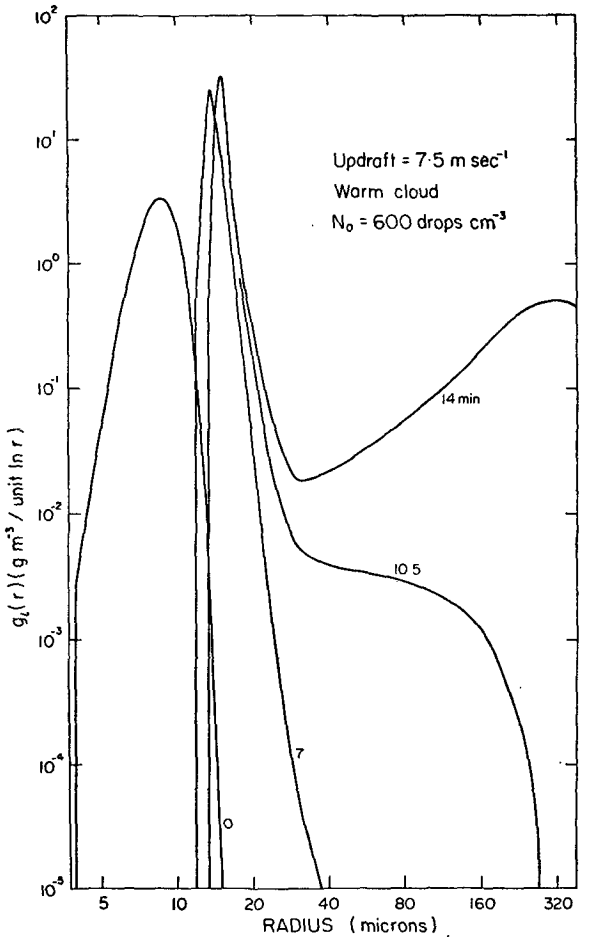

FIG. 4. Mass distribution after 0, 7, 10.5 and 14 min, corresponding to heights above cloud base of 0.7, 3.8, 5.3 and 7.0 km, for an updraft of 7.5 m sec^{-1} in the warm cloud. The initial number distribution is shown in Fig. 3.

scribing the rate of change of $N(x)$ is given by

$$\frac{\partial N(x)}{\partial t}=\int_0^{x/2} dx' N(x_c)V(x_c,x')N(x') - \int_0^{\infty} dx' N(x)V(x,x')N(x'), \quad (1)$$

where $V(x,x')$ is the collection kernel and $x_c=x-x'$. The first term is the rate of change of $N(x)$ due to collisions between pairs of droplets whose masses add to x, and the second term the rate at which droplets of mass x are lost due to collisions with other droplets. The statement of the coalescence problem in this form is due to Melzak and Hitschfeld (1953).

Berry (1967) was able to express Eq. (1) in a form particularly suitable for numerical solution by introduring a computation parameter J defined by the equation

$$x(J)=x_0 \exp[3(J-1)/J_0].$$

With J assuming values from 1 to 81, $x_0=2.58\times10^{-10}$ gm, and $J_0=12/\ln 2$, the droplet radius $r(J)$ takes values from 3.94 to 400 μm, doubling every 12 categories. The sensitivity of the solution of (1) to various numerical methods has recently been pointed out by Reinhardt (1972) and it is his interpolation and integration techniques that we have followed. Thus, a mass density function $M(x)$ is defined by

$$M(x)=xN(x),$$

where $M(x)dx$ is the mass of the drops, per unit volume of cloudy air, in the interval dx.

In terms of J, the mass density function becomes

$$g(J)=M(x)\frac{dx}{dJ}=xN(x)\frac{3x}{J_0}. \quad (2)$$

For the purposes of displaying the results it is convenient also to introduce a log-increment density function $g_L(r)$, defined by $g_L(r)d\ln r=g(J)dJ$. Thus, $g_L(r)=3x^2N(x)$.

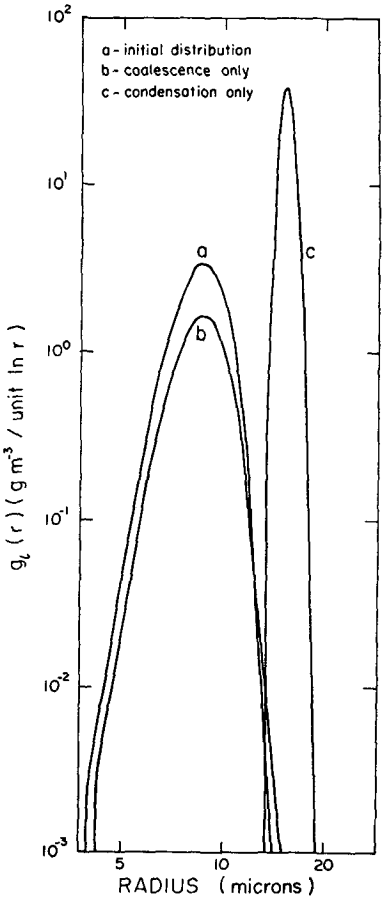

FIG. 5. Mass distribution for the same conditions as in Fig. 4. Curve (a) is the initial distribution, (b) the result after 14 min of coalescence but no condensation, and (c) the spectrum after 14 min of condensation but no coalescence. The liquid water contents are 1.3, 0.6 and 4.0 gm m^{-3}, respectively.

Unauthenticated | Downloaded 06/13/24 11:36 AM UTC

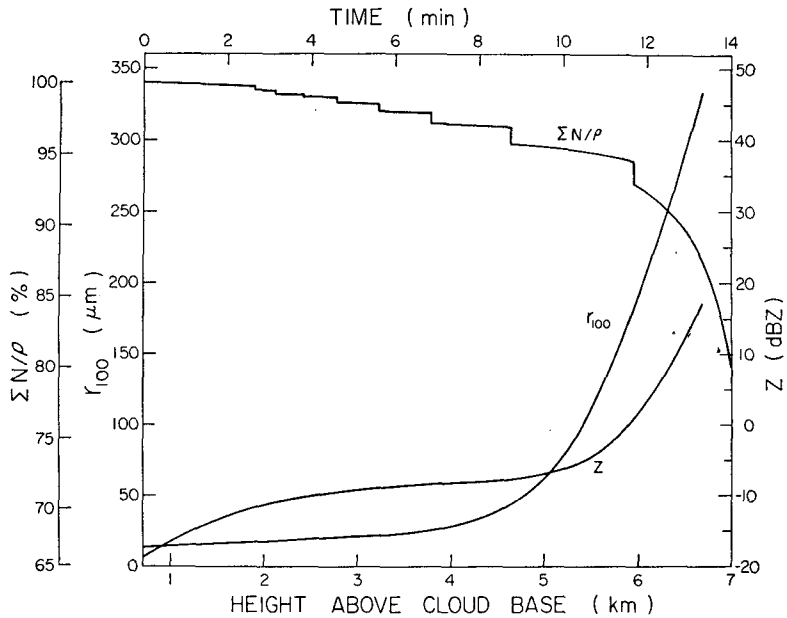

FIG. 6. The droplet mixing ratio (N/ρ) as a percentage of the initial value, the radius of the 100th largest drop per cubic meter (r_{100}), and the radar reflectivity factor Z as functions of the height of the parcel above cloud base (or time), corresponding to the results of Fig. 4.

Eq. (2) can be used to write (1) in the form

$$\frac{\partial g(J)}{\partial t}=x(J)\left\{\int_1^{J_d}\frac{x(J)}{x(J_c)}g(J_c)W(J_c,J')g(J')dJ' - \int_1^{\infty} g(J)W(J,J')g(J')dJ'\right\}, \quad (3)$$

where J_c is defined by $x_c=x_0\exp[3(J_c-1)/J_0]$ and J_d by $x(J)/2=x_0\exp[3(J_d-1)/J_0]$; $W(J,J')$ is a modified collection kernel related to $V(x,x')$ by

$$W(J,J')=V[x(J),x(J')]/[x(J)x(J')].$$

Since J_c, in general, is not an integer, $g(J_c)$ must be determined by interpolation. Reinhardt has found that a six-point Lagrange interpolation on the natural logarithm of $g(J)$ was most accurate. The same interpolation scheme was used on $W(J,J')$ to determine the values of $V(J_c,J')$. As a measure of the accuracy of the methods used, in the worst case considered here the total change in water content due to errors in solving the coalescence equation was less than 0.2% over a time interval of 12 min. The time integration of (3) was by forward differences with a time step of 1 sec. Reducing the time step to 0.5 sec produced a negligible change.

Values of the fall velocities were taken from Stokes' law for radii <25 μm and from the drag measurements of Beard and Pruppacher (1969) for larger radii. In order to avoid recalculating the kernels for different air densities a simple $\rho_{\text{air}}^{1/3}$ dependence was assumed.

Collision efficiencies were interpolated from the results of Shafrir and Neiburger (1963) for pairs of drops for which the radius of the larger drop was greater than 30 μm, and from Hocking and Jonas (1970)[1] for pairs in which both droplets had radii $\leqslant 30$ μm. Fig. 1 shows the values of the product of collision efficiency Y_c^2, as defined by Shafrir and Neibruger, times the fall velocity difference.

c. Condensation

Droplet growth by condensation is modeled by the simplest form of the diffusional growth equation:

$$\frac{dr}{dt}=\frac{c}{r}, \quad (4)$$

where

$$c=(S-1)\left[\frac{L^2\rho_L}{KR_vT^2}+\frac{R_vT\rho_L}{De_s(T)}\right]^{-1}, \quad (5)$$

with S the saturation ratio, L the latent heat of vaporization, ρ_L the density of water, R_v the gas constant for water, T the temperature, K the coefficient of thermal conductivity of air, D the diffusion coefficient of water vapor in air, and $e_s(T)$ the equilibrium vapor pressure.

If $n(r,t)dr$ denotes the number of droplets per unit volume of air with radii in dr at time t, then it follows from (4) that at time $t+\Delta t$ the spectrum will have

[1] The results corresponding to a critical separation of 10^{-3} of the larger drop radius were used.

Unauthenticated | Downloaded 06/13/24 11:36 AM UTC

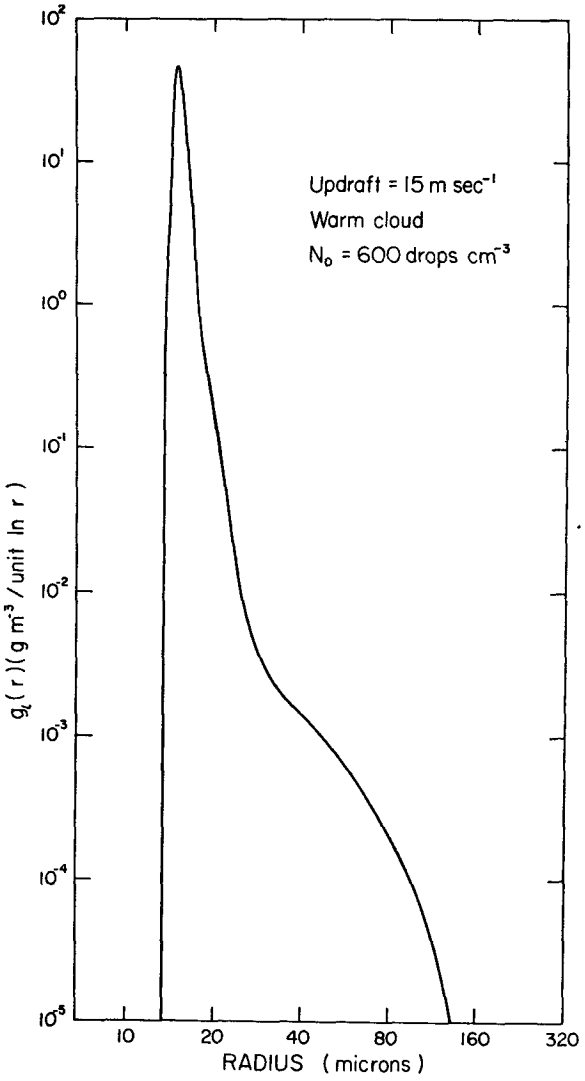

FIG. 7. Mass distribution after 7 min for an updraft of 15 m sec^{-1} in the warm cloud and the initial distribution shown in Fig. 3.

evolved, by condensation only, to the form

$$n(r, t+\Delta t)=r(r^2-2c\Delta t)^{-\frac{1}{2}}n[(r^2-2c\Delta t)^{\frac{1}{2}}, t] \times\frac{\rho(t+\Delta t)}{\rho(t)}, \quad (6)$$

where $\rho(t)$ is the density of the air at time t. This result follows from the assumption that the droplet mixing ratio remains constant during Δt. It may be shown to be a special case of the general solution formulated by Kovetz (1969). In terms of the mass distribution function, (6) becomes

$$g[J(r), t+\Delta t]=r^5(r^2-2c\Delta t)^{-\frac{5}{2}}g[J(r^2-2c\Delta t)^{\frac{1}{2}}, t] \times\frac{\rho(t+\Delta t)}{\rho(t)}. \quad (7)$$

In the calculations c is determined not from the thermodynamic relation (5), but from the requirement that the condensed water content at any altitude equal the adiabatic value. Then (5) may be used to solve for the supersaturation $(S-1)$.

In principle, the time interval Δt would be chosen with no restriction other than it be short enough to insure that the change in the spectrum due to condensation has negligible effect on the rate of coalescence. Then the liquid water content resulting from saturated adiabatic expansion, the value of c, and incidentally $(S-1)$ could be determined. However, for an arbitrary choice of Δt the minimum radius in the new distribution, $r_{\min}$, would not, in general, correspond to an integral value of J. This would complicate the coalescence calculations. The problem is circumvented by reversing part of the procedure. Thus, at each time step several values of c are considered, each of which allows $r_{\min}$ to correspond to an integral value of J. The correct value of c for a given time step is then chosen as the one for which the liquid water content, obtained by integrating (7), corresponds most closely to the adiabatic value. Consequently, $r_{\min}$ always corresponds to an integral J but the actual liquid water content oscillates about the adiabatic value. An example of the way the water content approximates the adiabatic value is shown in Fig. 2. The approximation is best initially, where the mass difference between adjacent values of J is small, and gets worse as $r_{\min}$ increases.

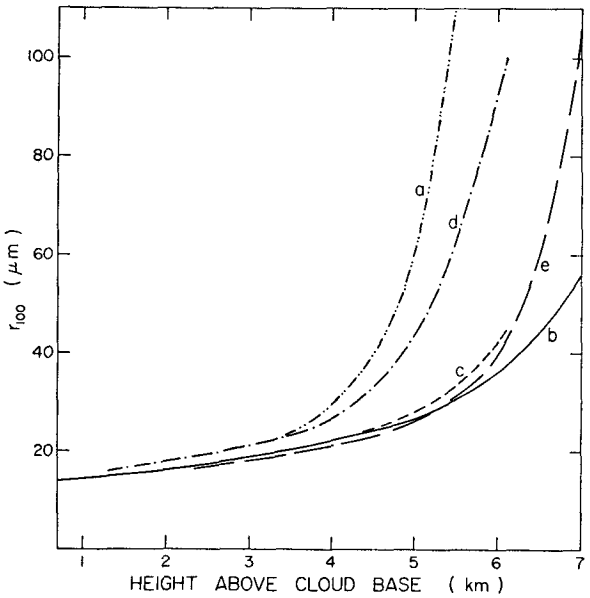

FIG. 8. The radius r_{100} of the 100th largest drop per cubic meter as a function of the height above cloud base. The cloud temperatures, updrafts, and initial droplet concentrations are: (a) warm, 7.5 m sec^{-1}, 600 cm^{-3}; (b) warm, 15 m sec^{-1}, 600 cm^{-3}; (c) cold, 7.5 m sec^{-1}, 600 cm^{-3}; (d) cold, 7.5 m sec^{-1}, 450 cm^{-3}; (e) warm, 7.5 m sec^{-1}, 900 cm^{-3}.

Unauthenticated | Downloaded 06/13/24 11:36 AM UTC

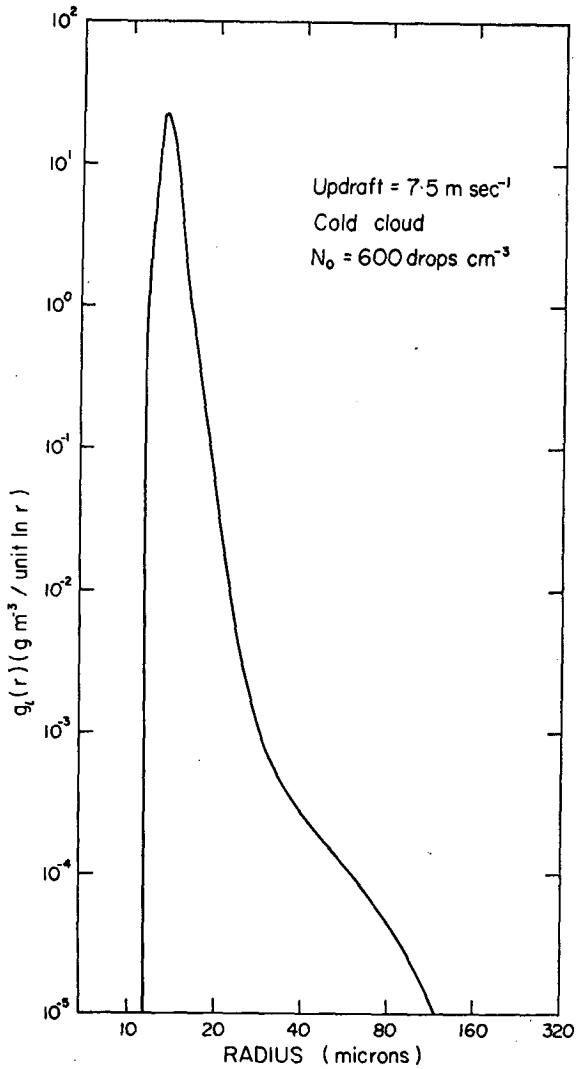

FIG. 9. Mass distribution after 11.5 min, corresponding to a height 6.0 km above cloud base, for an updraft of 7.5 m sec^{-1} in the cloud. The initial distribution is shown in Fig. 3 and originated at a height 0.9 km above cloud base.

3. Initial conditions

The calculations require specification of the pseudo-adiabat describing the ascent of the cloud parcel. This has been done in terms of a cloud base height and temperature, assuming a standard atmosphere. The height of cloud base was fixed at 2300 m (MSL) and calculations were carried out for cloud base temperatures of 10 and 4.5C (referred to as the warm cloud and cold cloud, respectively). In terms of the wet bulb potential temperature, $\theta_w = 293.5$K for the warm cloud and 289K for the cold cloud. These are representative conditions for severe and moderate hailstorms in Alberta.

Most of the calculations are for a constant updraft of 7.5 m sec^{-1} although the effect of increasing the updraft to 15 m sec^{-1} is considered. The results for a weak updraft of 0.5 m sec^{-1} were also calculated as a separate case.

The initial distributions are of the form used by Scott (1968a). In terms of $g(J)$ they may be written

$$g(J)=\frac{3N_0}{J_0}\frac{(\nu+1)^{\nu+1}}{\Gamma(\nu+1)}\frac{x^{\nu+2}}{\bar{x}^{\nu+1}}\exp[-(x/\bar{x})(\nu+1)],$$

where N_0 is the total number of drops per unit volume, $\bar{x}$ the mean mass of the distribution, and ν a measure of the spectrum width. The value of ν was kept fixed at 3 which resulted in a relative dispersion in $n(r)$ of $\sigma_r/\bar{r}\approx 0.2$. With the exception of two cases discussed in the following section, $\bar{x}=2.15\times10^{-9}$ gm, corresponding to radius $r_{\bar{x}}=8$ μm. The values of these parameters are consistent with values measured by MacCready

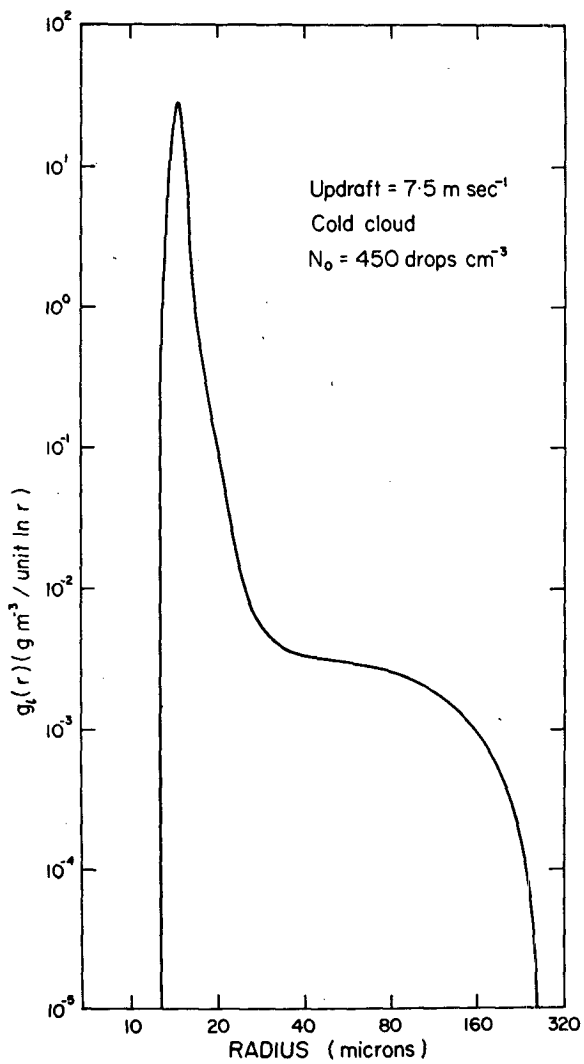

FIG. 10. Mass distribution after 12 min, corresponding to a height of 6.0 km above cloud base, for an updraft of 7.5 m sec^{-1} in the cold cloud. The initial distribution had the same shape as the distribution of Fig. 3 but with 450 drops cm^{-3}, and originated at a height 0.6 km above cloud base.

Unauthenticated | Downloaded 06/13/24 11:36 AM UTC

and Takeuchi (1968) a few hundred meters above cloud base. A plot of the standard initial distribution with $N_0=600$ drops cm^{-3} and the above values of ν and $\bar{x}$, resulting in a water content of 1.3 gm m^{-3}, is given in Fig. 3. The effect of varying N_0 is also discussed below.

Instead of starting the calculations at cloud base, they were begun at the height where the water content contained in the initial droplet spectrum was equal to the adiabatic value. Accordingly, the initial height varied from 350 m to 1150 m above cloud base, depending on the water content of the initial spectrum and whether the warm or cold cloud was being considered.

4. Results

Fig. 4 shows the development of the distribution given in Fig. 3, in terms of the function $g_L(r)$, at different times, for the warm cloud and an updraft of 7.5 m sec^{-1}. The calculation was terminated after 14 min of ascent, the time for the parcel to reach the −40C level. At this height the liquid water content was ~4 gm m^{-3}. A narrow "condensation peak" forms very quickly and gradually a "coalescence tail" starts to form. The mass in the tail of the spectrum increases at an accelerating rate, but not to the extent that it destroys the condensation peak. At no time in the development does the spectrum have the shape of the droplet distributions that have generally been used to initiate coalescence calculations (e.g., Berry, 1967; Cotton, 1972). Fig. 5 shows the results of similar calculations in which (i) only coalescence but no condensation, and (ii) only condensation but no coalescence were assumed to take place. It is not surprising, in view of the results of Bartlett and Reinhardt, that the coalescence calculation alone does not produce precipitation size drops in a period of 14 min when starting from the initial distribution used here. However, including growth by condensation results in a distribution that can grow rapidly by coalescence as shown by Fig. 4. A significant number of drops with radius >100 μm are produced by the time the parcel reaches the −40C level.

The development of the distribution is indicated in Fig. 6 by showing the changes of the radar reflectivity factor Z and the radius r_{100} of the 100th largest drop per cubic meter, as functions of height above cloud base. Introduced by Twomey (1966), r_{100} is such that 100 drops m^{-3} are larger than or equal to r_{100}. Both of these parameters give indications of the height at which coalescence is starting to become important, with r_{100} being the more sensitive. At the point where the calculations were terminated r_{100} was greater than 340 μm and the reflectivity was greater than 16 dBZ, a value that would be detectable at close range for most weather radars. The supersaturation was determined at various times from the values of c in (5) and

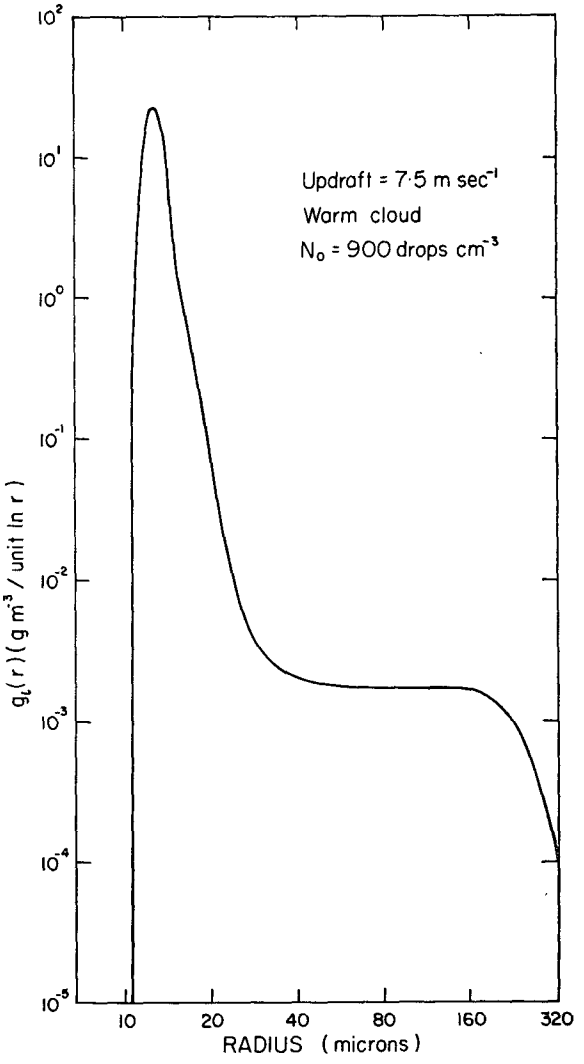

FIG. 11. Mass distribution after 13 min, corresponding to a height of 7.1 km above cloud base, for an updraft of 7.5 m sec^{-1} in the warm cloud. The initial distribution had the same shape as the distribution of Fig. 3 but with 900 drops cm^{-3}, and originated at a height 1.1 km above cloud base.

the time between condensation steps, the results falling within the range 0.25 to 0.45%.

Also included in Fig. 6 is a plot of the droplet mixing ratio $\Sigma N/\rho$. The discontinuities in the curve are an indication of errors in the numerical integrations to determine the number of drops before and after condensation steps. It is not surprising that these should occur in view of the very sharp nature of the condensation peak (Fig. 4). The rapid but smooth decrease in the droplet mixing ratio above about 6 km is another indication that coalescence has become important.

The effect of increasing the updraft speed to 15 m sec^{-1} is shown in Fig. 7. As expected, the total mass contained in the large droplets has been reduced owing to the shorter time available for coalescence to take place. (The calculation was again terminated when the

Unauthenticated | Downloaded 06/13/24 11:36 AM UTC

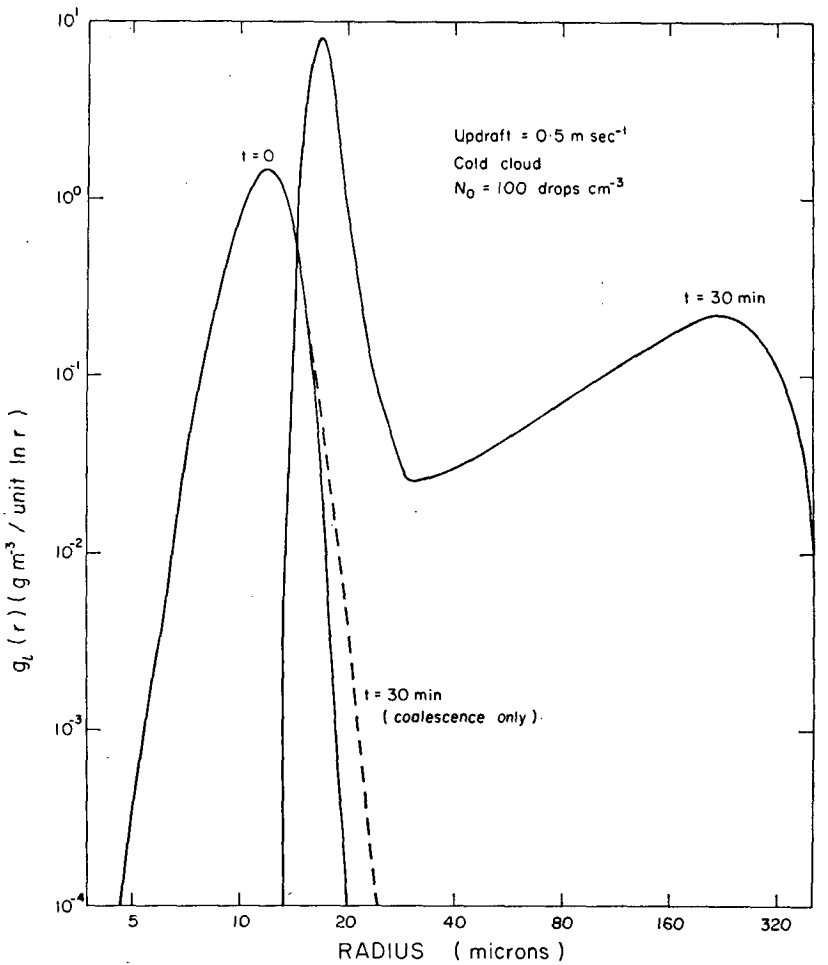

FIG. 12. Mass distribution after 30 min for an updraft of 0.5 m sec^{-1} in the cold cloud. The dashed curve is the result of a calculation in which all condensation and density effects were suppressed. The initial distribution is specified in the text.

parcel temperature reached −40C.) Fig. 8 (curve b) shows the growth of r_{100}. In this case the maximum value attained was 56 μm. The radar reflectivity factor was found to exhibit no significant increase.

The cold cloud has a maximum liquid water content of 3 gm m^{-3}. The effect of this reduction on the development of the distribution is shown in Figs. 8 (curve c) and 9 for an updraft of 7.5 m sec^{-1}. The growth of the spectrum is now markedly reduced compared to the corresponding calculation for the warm cloud (Figs. 4 and 6), r_{100} attaining a maximum value of 46 μm at just above 6 km, where the temperature is −40C.

The results of repeating the calculations for the 7.5 m sec^{-1} updraft in the cold cloud but with the number of drops in the initial distribution reduced from 600 to 450 cm^{-3}, leaving the mean radius and dispersion unchanged, are shown in Fig. 8 (curve d) and Fig. 10. The number of drops with radii >100 μm is now significantly increased. This results from a faster condensation growth rate leading to an earlier onset of rapid coalescence.

The opposite effect is shown in Fig. 11 for a 7.5 m sec^{-1} updraft in the warm cloud, with N_0 increased to 900 drops cm^{-3}, leaving the mean radius and dispersion unchanged. Here the condensation growth rate has been diminished with the result that rapid coalescence has been delayed. The initial distribution in this case had a rather high water content (1.9 gm m^{-3}); to make the initial conditions more consistent with previous examples, another calculation was carried out with an initial drop size distribution having the same dispersion but radius $r_{\bar{x}}$ reduced from 8 to 7 μm. With 900 drops cm^{-3} this results in a total mass of 1.3 gm m^{-3}, the same as that of the standard distribution with 600 drops cm^{-3}. The results of this calculation (not shown) were almost indistinguishable from those of Fig. 11 for the high water content.

In addition to the above calculations for strong updraft conditions a calculation was performed for a gentle updraft of 0.5 m sec^{-1} in the cold cloud and a maritime type initial distribution. The shape of the initial spectrum was the same as above with the dispersion $\sigma_r/\bar{r}=0.2$ but with $r_{\bar{x}}=11$ μm and $N_0=100$

Unauthenticated | Downloaded 06/13/24 11:36 AM UTC

cm^{-3}, corresponding to a total mass of 0.56 gm m^{-3}. The development of the distribution in ascending for 30 min is sufficiently rapid that appreciable concentrations of drizzle drops have formed (Fig. 12). For such a gentle updraft it is not valid to neglect droplet fallout. Although the results must consequently be accepted with caution, the importance of condensation combined with coalescence is clearly indicated in Fig. 12.

5. Concluding remarks

The approach taken here has been to start with a cloud droplet spectrum typical of what has been measured at cloud base and to calculate the development of the spectrum as the cloud parcel rises. This leads to a narrow condensation peak and eventually to a second peak in the mass density function due to growth by coalescence.

Growth by coalescence alone, starting from realistic continental droplet spectra, does not lead to the formation of precipitation in times consistent with observations of showers. However, if condensation is included, development can be sufficiently rapid that within 15 min large numbers of drizzle size drops will have formed, the distribution will be radar-detectable, and rapid growth to raindrop sizes would be expected.

In coalescence calculations (e.g., Berry 1967; Cotton, 1972) the tendency has been to start from an assumed condensation spectrum that contains an appreciable concentration of large droplets. The results found here indicate that such an assumption is unnecessary. In fact, the strong dependence of the development of the distribution on the condensation rate raises the question of the validity of the concept of autoconversion, which inherently assumes the separability of growth by condensation and growth by coalescence.

Acknowledgments. We are very grateful to Drs. E. X Berry and R. L. Reinhardt for sending us their results and coalescence program. This work was supported by the Atmospheric Environment Service of Canada.

REFERENCES

Bartlett, J. T., 1970: The effect of revised collision efficiencies on the growth of cloud droplets by coalescence. *Quart. J. Roy. Meteor. Soc.*, **96**, 730–738.

Beard, K. V., and H. R. Pruppacher, 1969: A determination of the terminal velocity and drag of small water drops by means of a wind tunnel. *J. Atmos. Sci.*, **26**, 1066–1072.

Berry, E. X, 1967: Cloud droplet growth by coalescence. *J. Atmos. Sci.*, **24**, 688–701.

Cotton, W. R., 1972: Numerical simulation of precipitation development in supercooled cumuli—Part 1. *Mon. Wea. Rev.*, **100**, 757–763.

Danielsen, E. F., R. Bleck and D. A. Morris, 1972: Hail growth by stochastic collection in a cumulus model. *J. Atmos. Sci.*, **29**, 135–155.

East, T. W. R., 1957: An inherent precipitation mechanism in cumulus clouds. *Quart. J. Roy. Meteor. Soc.*, **83**, 61–76.

Gillespie, D. T. 1972: The stochastic coalescence model for cloud droplet growth. *J. Atmos. Sci.*, **29**, 1496–1510.

Hocking, L. M., and P. R. Jonas, 1970: The collision efficiency of small drops. *Quart. J. Roy. Meteor. Soc.*, **96**, 722–729.

Kovetz, A., 1969: An analytical solution for the change of cloud and fog droplet spectra due to condensation. *J. Atmos. Sci.*, **26**, 302–304.

——, and B. Olund, 1969: The effect of coalescence and condensation on rain formation in a cloud of finite vertical extent. *J. Atmos. Sci.*, **26**, 1060–1065.

MacCready, P. B., Jr., and D. M. Takeuchi, 1968: Precipitation initiation mechanisms and droplet characteristics of some convective cloud cores. *J. Appl. Meteor.*, **7**, 591–602.

Melzak, A. Z., and W. Hitschfeld, 1953: A mathematical treatment of random coalescence. Sci. Rept. MW-11 Stormy Weather Group, McGill University, Montreal, 28 pp.

Reinhardt, R. L., 1972: An analysis of improved numerical solutions to the stochastic collection equation for cloud droplets. Ph.D. thesis, University of Nevada, 111 pp.

Scott, W. T., 1968a: Analytic studies of cloud droplet coalescence I. *J. Atmos. Sci.*, **25**, 54–65.

——, 1968b: Comments on "Cloud droplet coalescence: Statistical foundations and a one-dimensional sedimentation model." *J. Atmos. Sci.*, **25**, 150.

——, 1968c: On the connection between the Telford and kinetic equation approaches to droplet coalescence theory. *J. Atmos. Sci.*, **25**, 871–873.

Shafrir, U., and M. Neiburger, 1963: Collision efficiencies of two spheres falling in a viscous medium. *J. Geophys. Res.*, **68**, 4141–4147

Srivastava, R. C., 1971: Size distribution of raindrops generated by their breakup and coalescence. *J. Atmos. Sci.*, **28**, 410–415.

Takeda, T., 1971: Numerical simulation of a precipitating convective cloud: The formation of a "long-lasting" cloud. *J. Atmos. Sci.*, **28**, 350–376.

Twomey, S., 1966: Computations of rain formation by coalescence. *J. Atmos. Sci.*, **23**, 405–411.

Warshaw, M., 1967: Cloud droplet growth: Statistical foundations and a one-dimensional sedimentation model. *J. Atmos. Sci.*, **24**, 278–286.

——, 1968: Cloud droplet coalescence: Effects of the Davis-Sartor collision efficiency. *J. Atmos. Sci.*, **25**, 874–877.

Unauthenticated | Downloaded 06/13/24 11:36 AM UTC